Development 127, 3395-3405 (2000)
Printed in Great Britain © The Company of Biologists Limited 2000
DEV3190

The *eli1* mutation reveals a link between cell expansion and secondary cell wall formation in *Arabidopsis thaliana*

Ana I. Caño-Delgado, Karin Metzlaff and Michael W. Bevan*

Department of Molecular Genetics, John Innes Centre, Norwich Research Park, Colney Lane, Norwich, NR4 7UH, UK
*Author for correspondence (e-mail: michael.bevan@bbsrc.ac.uk)

Accepted 19 May; published on WWW 10 July 2000

SUMMARY

Mutants with altered patterns of lignification have been identified in a population of mutagenised Arabidopsis seedlings. One of the mutants exhibited *e*ctopic *li*gnification *(eli)* of cells throughout the plant that never normally lignify. The reduced expansion of *eli1* cells resulted in a stunted phenotype, and xylem cells were misshapen and failed to differentiate into continuous strands, causing a disorganized xylem. Analysis of phenotypes associated with double mutants of *eli1 lit* (*lion's tail*), a cell expansion mutant, indicated that the primary defect in *eli1* plants may be inappropriate initiation of secondary wall formation and subsequent aberrant lignification of cells caused by altered cell expansion. Related ectopic lignification phenotypes were also observed in other cell expansion mutants, suggesting a mechanism that senses cell size and controls subsequent secondary wall formation. Interactions between *eli1* and *wol* (*woodenleg*), a mutant altering xylem cell specification, revealed a role for *ELI1* in promoting formation of continuous xylem strands, and demonstrated that *ELI1* functions during cell elongation zone in the primary root and other tissues.

Key words: *Arabidopsis thaliana*, Cell wall, Cell expansion mutants, Secondary thickening, Lignification, *ELI1*

INTRODUCTION

The formation and differentiation of the cell wall plays a key role in plant morphogenesis. Two general types of plant cell walls can be distinguished: a thin primary wall which is synthesized during cell expansion and is capable of yielding to turgor pressure (Cosgrove, 1993), and a secondary, thicker wall deposited in the fully expanded cell between the primary wall and the plasma membrane. Secondary wall formation is restricted to specialized cells and provides mechanical strength and rigidity to support aerial structures and hydrophobicity for transport functions.

Several models of the organization of the plant cell wall have described the arrangement of the primary wall components and their structural modification during cell expansion (reviewed by Carpita and Gibeaut, 1993; McCann and Roberts, 1994; Cosgrove, 1999). The plant primary cell wall is mainly composed of cellulose microfibrils and a polysaccharide matrix of hemicellulose, pectins and proteins. The organization of cellulose microfibrils and their complex interaction with other cell wall components results in an extensive and dynamic network that can be modified by the action of several cell-wall enzymes, such as endoglucanases, xyloglucan-endotransglycoxylases and expansins (reviewed by Cosgrove, 1999). These proteins contribute to the continuous breaking and remaking of bonds necessary to maintain the integrity of the cell wall during cell expansion. The isolation and characterization of genes involved in the synthesis of major cell wall polysaccharides (Pear et al., 1996; Bonin et al., 1997; Turner and Somerville, 1997; Taylor et al., 1999; Arioli et al., 1998; Nicol et al., 1998) is starting to reveal the mechanisms of primary cell wall formation.

The formation of secondary cell walls has been studied most intensively during the development of xylem cells. This process is characterized by deposition of lignin into a matrix of polysaccharides (Roberts, 1989), and subsequent loss of cellular contents (Wardrop, 1981; O'Brien, 1981). The expression of specific genes associated with different stages of xylogenesis has been catalogued in differentiating *Zinnia* mesophyll cells. For example, genes encoding proteins involved in remodeling the endomembrane system in preparation for secondary thickening of the longitudinal walls, in the synthesis of lignin precursors and in lysis of cell contents have been identified (Fukuda et al., 1994).

The mechanisms governing the spatial and temporal patterns of secondary wall formation are beginning to be understood. Mutants defective in aspects of vascular development have been identified in *Arabidopsis*, for example the *wooden leg* (*wol*) mutant (Scheres et al., 1995), which fails to establish the appropriate numbers of vascular cells, and *lion's tail* (*lit*),which is impaired in the radial expansion of vascular cells (Hauser et al., 1995). Mutants altered in different aspects of polysaccharide synthesis and secondary wall deposition have also been identified. An interfascicular fiberless mutant (*ifl1*) is disrupted in normal development of interfascicular fibres in *Arabidopsis*, leading to flaccid, mechanically weak stems

(Zhong et al., 1997). The *IFL1* gene encodes a homeodomain-leucine-zipper protein (Zhong and Ye, 1999). The irregular xylem (*irx*) mutants are characterized by a reduction in cellulose in stem tissue, primarily associated with xylem cells (Turner and Somerville, 1997). *IRX3* encodes a catalytic subunit of a cellulose synthase complex specifically required for the synthesis of cellulose in the secondary cell wall (Taylor et al., 1999).

We have screened for mutants exhibiting abnormal patterns of lignification in the primary root of *Arabidopsis*. We report the isolation and characterization of one of these mutants, termed *eli1* (*e*ctopic *li*gnification 1) and describe a role for the *ELI1* gene in integrating cell expansion and secondary cell wall formation.

MATERIALS AND METHODS

Plant material and growth conditions

The *Arabidopsis thaliana* ecotype Columbia (Col) was used for mutant isolation. The *lion's tail* (*lit*), *cobra* and *pom-pom* Col seeds (Hauser et al., 1995) were provided by Maria-Theres Hauser, *wol* Col seeds (Scheres et al., 1995) by Philip Benfey, *kor1* WS seeds (Nicol et al., 1998) were provided by Herman Höfte, *rsw1* Col seeds (Baskin et al., 1995) by Keith Roberts, and *det3* Col seeds (Cabrera y Poch et al., 1993) by Joanne Chory.

Seeds were surface sterilized in 5% sodium hypochlorite, rinsed with sterile water and plated in 1× MS salts (Murashige and Skoog,) containing 30 mM or 100 mM sucrose, 0.3% phytagel (pH 5.8), and imbibed at 4°C for 48 hours in darkness. Seedlings were grown in a vertical position in continuous light (80 μeinsteins/m^2/second) at 21°C. After 7 days plants were transferred to soil and grown in a greenhouse. rsw1 seeds were grown at 21°C for 5 days and transferred to 31°C for a further 2 days to express the conditional phenotype.

Seedlings were grown as described above on media supplemented with different concentrations of indole-3-acetic acid (IAA) and kinetin (0.5 nM, 50 nM, 0.5 μM and 5 μM), epi-brassinosolide (1 μM) and gibberellin GA4 (10^{-4} M and 10^{-5} M). For ethylene response assays seedlings were germinated on either 10^{-4} M ACC or 10^{-4} M silver nitrate. Root phenotypes were analysed 7 days after germination.

The Landsberg erecta (L*er*) ecotype was used for mapping.

Mutagenesis and screening

Col seeds were treated with 0.5% ethyl methane sulphonate (EMS) in water for 8 hours at 22°C, and sown on soil for growth in the greenhouse. Single siliques representing a total of 4,000 M_2 families were harvested. An additional 1800 families containing multiple copies of an autonomous En transposon (Wisman et al., 1998) were used in the same screen. A total of 87,000 M_2 seeds were plated in 4,000 individual families and grown on vertical plates for 7 days before screening. The screen for mutants with altered lignin distribution was carried out in seedlings in chloral hydrate:glycerol:distilled water (8:1:2) (Berleth and Jürgens, 1993). Cleared seedlings were stained and mounted with a saturated solution of phloroglucinol:HCl and viewed under dark-field illumination. Siblings from segregating populations were kept and their progeny re-tested in the M_3 generation.

Genetics and mapping

The *eli1* mutant was back-crossed twice to wild-type Columbia, and progeny of the final back-cross were used for subsequent experiments. The F_1 progeny of crosses between all three alleles of *eli1* and Col wild type were phenotypically wild type, while the F_2 progeny from self-pollinated F_1 showed a segregation ratio of 3:1 for wild-type:mutant phenotype for the three isolated alleles of *eli1* (251 *ELI1-1/+*, 79 *eli1-1/eli1-1*, χ^2=2.4, *P*>0.05; 301 *ELI1-2*/+, 87 *eli1-2/eli1-2*; χ^2=1.37, *P*>0.05; and 287 *ELI1-3*/+, 92 *eli1-3/eli1-3*; χ^2=0.09, *P*>0.05), indicating that *eli1* is a single locus, nuclear recessive mutation. Double mutants between *eli1* and *lit*, and *eli1* and *wol* mutants were obtained by crossing plants homozygous for the mutations and screening the F_2 progeny.

The *eli1* mutant was crossed to Landsberg *erecta* (L*er*) and segregating F_2 populations were prepared for mapping with simple sequence length polymorphism (SSLP) markers as described by Bell and Ecker (1994). Each marker was tested on the DNA of 90 single *eli1* seedlings from the segregating F_2 of these crosses.

Histology

Transverse sections (2 μm) of the primary root were made in Historesin-embedded material as described by Schneider et al. (1997) and stained with 0.05% Toluidine Blue O (Sigma) for 30 seconds. Inflorescence stem sections were cut by hand and stained with 0.05% Toluidine Blue O for 1 minute, rinsed and mounted in water. Cell wall material was stained with 0.001% Calcofluor in semi-thin sections.

Confocal scanning laser microscopy

Roots of 7-day-old seedlings were cleared with methanol for 1 hour at room temperature, and then with 10% NaOH at 60°C for 12 hours, and stained with 0.01% basic Fuchsin to visualize lignin (Dharmawardhana et al., 1992). Optical sections in the longitudinal plane were made using a Bio-Rad MRC-1024 Confocal Scanning Laser Microscope (CSLM). To image all xylem vessels, Z-series were captured and stacked using the NIH-image programme.

Scanning electron microscopy

Seven-day-old seedlings were mounted on the surface of an aluminium stub with OCT compound, immersed into liquid nitrogen slush, and put onto the cold stage of a CT1500HF cryotransfer system attached to a Phillips XL30 FEG scanning electron microscope. Sublimation was performed at –95°C for 3 minutes before sputter-coating the sample with platinum for approximately 2 minutes at 10 mA.

Immunolabelling and electron microscopy

For transmission electron microscopy (TEM), 7-day-old root tissues were fixed in 4.5% formaldehyde, dehydrated in an ethanol series, and infiltrated in LR White resin as described by Wells (1985). Rabbit polyclonal antibodies against lignin dehydrogenation polymer (GSzt L4, mixed anti-guaiacyl-syringyl lignin) were used (Joseleau and Ruel, 1997). Ultrathin tissue sections were blocked with 1% BSA and Tween 20, and treated with a 1/30 dilution of the primary antibody in 0.1% BSA and incubated for 3 hours. Sections were washed three times with PBS pH 7.4 for 10 minutes before incubation for an hour with the secondary antibody (10 nm gold-goat anti-rabbit, BioCell) diluted in 0.1% BSA. Sections were then post-fixed in 1% glutaraldehyde, stained with 2% uranyl acetate and alkaline lead citrate, and observed on a JEOL 1200 electron microscope. Semi-thin sections were used for immunofluorescence detection of lignin with a secondary cy3-labelled goat anti-rabbit antibody diluted 1/100 in 0.1% BSA. Sections were incubated for 3 hours. Pre-immune antisera and the omission of the primary antibody were used as immunochemical controls.

Images were composed using Adobe® Photoshop 5.0.

RESULTS

Screening procedure

A total of 4,000 individual M_2 EMS families and 1800 En transposon insertion lines were screened for altered patterns of lignification. In wild-type tissues, secondary thickened xylem

cells are lignified, therefore the pattern of phloroglucinol staining can reveal alterations in secondary wall deposition and alterations in xylem development.

Isolation of mutants with altered patterns of lignification

Three groups of mutants were identified on the basis of patterns of phloroglucinol staining in the primary root. *mux* (multiple xylem) mutants exhibited an increased number of xylem strands in the primary root, *tpx* mutants displayed an altered timing of protoxylem development in the primary root, and *eli* (ectopic lignification) mutants exhibited an altered pattern of lignification. The *mux* and *tpx* mutants isolated were the result of monogenic recessive mutations. All the mutants with altered xylem development resulted in a shortened root system.

Three ectopic lignification mutant lines, two from the EMS mutagenized population and one from the En transposon lines, were identified. They exhibited essentially the same phenotype, with a characteristic lignification pattern in the primary root. The three mutants belong to the same complementation group, therefore they were designated *eli1-1* and *eli1-2* (the EMS mutagenized lines alleles) and *eli1-3* (the En transposon insertion line allele). The first line identified, *eli1-1*, was used for all the subsequent studies. Using a population of 90 F_2 *eli1-1* seedlings in crosses with wild-type L*er*, the *eli1* locus was found to map to the short arm of chromosome 5, between CTR1 and the SSLP marker nga249 (Bell and Ecker, 1994).

eli1 is characterised by reduced cell expansion and altered lignification

Light-grown 7-day-old *eli1* seedlings exhibited a primary root approximately 3 times shorter and thicker than the wild type (Table 1; Fig. 1A). Scanning electron microscopy (SEM) of the primary root revealed that epidermal cells of *eli1* (Fig. 1E) were shorter than wild-type cells (Fig. 1D), and they exhibited irregular, often bulbous protrusions. The *eli1* primary root had a reduced elongation zone with shorter cells, evident by the early appearance of root hairs in the differentiation zone (Fig. 1E). *eli1* lateral roots showed a similar shortened phenotype to the primary root, and fewer lateral roots were formed compared to wild type (data not shown). *eli1* seedlings stained with phloroglucinol exhibited an abnormal lignification pattern, with a higher than normal staining of lignin in the xylem strands, and a patchy mosaic of intense lignin staining in non-vascular cells (Fig. 1B). This staining pattern was observed in other tissues but was most intense in the root.

To determine the initial appearance of ectopic lignification, different developmental stages of *eli1* and wild-type embryos were stained with phloroglucinol and observed by light microscopy. No lignin staining was detected in embryos of wild-type and *eli1* plants (data not shown), indicating that the defect in *eli1* occurs in postembryonic tissues.

Since ectopic lignification was associated with reduced cell elongation, the *eli1* mutant was subjected to conditions that increased cell elongation in wild-type seedlings. Seven-day-old dark-grown *eli1* seedlings displayed a shorter hypocotyl and roots with shorter cells than wild type grown under the same conditions (Table1; Fig. 1C).

eli1 seedlings developed into mature plants which had a stunted aerial phenotype with reduced apical dominance, small leaves, siliques and flowers (Fig. 2A,B), suggesting that the cell expansion defect in *eli1* occurs in several tissues and organs. The reduced stamen elongation observed may account for the decreased fertility of *eli1* plants.

Patterns of lignification in *eli1*

Transverse sections of the primary root of Col and *eli1* seedlings revealed an abnormal cellular organization in *eli1* mutant plants (Fig. 3). All the cell layers of the *eli1* primary root were present, but radial cell expansion was increased (Fig. 3B) compared to the wild type (Fig. 3A). In the stele the number of cells differentiating into tracheids was higher in *eli1*

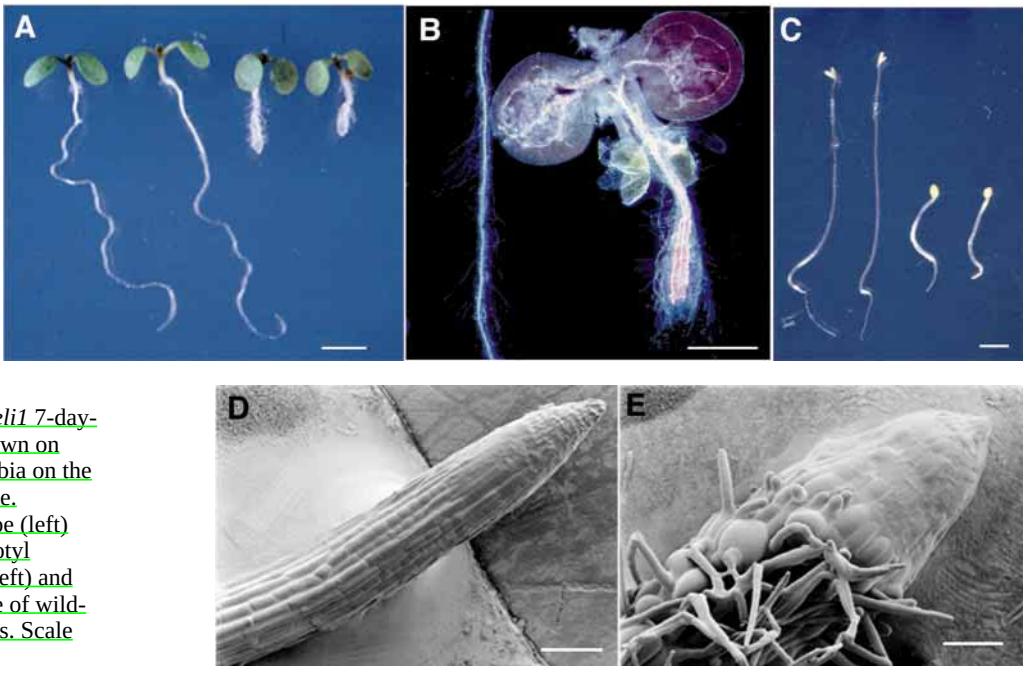

Fig. 1. Phenotypes of Columbia and *eli1* 7-day-old seedlings. (A) Seedlings were grown on vertical plates, with wild-type Columbia on the left and *eli1* seedlings on the right side. (B) Phlorolucinol staining of wild-type (left) and *eli1* (right) seedlings. (C) Hypocotyl elongation in darkness in wild-type (left) and *eli1* (right) seedlings. (D) SEM image of wild-type and (E) *eli1* mutant primary roots. Scale bars, 1 cm (A-C) and 100 μm (D,E).

Table 1. Root and hypocotyl length and lignin content of *eli1*, *lit* and *eli1 lit* mutants

		Genotype							
		Wt Col		*eli1*		*lit*		*eli1 lit*	
Tissue	Sucrose	Length (mm)	Lignin	Length (mm)	Lignin	Length (mm)	Lignin	Length (mm)	Lignin
Root	30 mM	12.61±1	–	3.96±0.2	++	6.12±0.2	+	1.69±1	+++
	100 mM	9.73±0.86	–	3.27±0.69	++	3.55±0.26	++	1.00±0.1	++
Hypocotyl	30 mM	9.30±0.73	–	3.56±0.62	+	5.80±1.10	–	0.64±0.47	+++

Lignin content was assessed using phloroglucinol staining. *n*=20.

(Fig. 3G,H) than in wild type (Fig. 3A,B). The number and position of the additional xylem elements in *eli1* changed from one section to another (as shown in Fig. 3E and F compared with 3G and H) suggesting that they were isolated tracheids that failed to form files of continuous cells.

Lignification in the primary root of *eli1* is not restricted to the xylem cells, as in wild-type plants, but also occurred in other vascular, pericycle, cortical or endodermal cells, as indicated by arrowheads in Figs 3F and 3H. This ectopic lignification appeared as amorphous patches of differing intensities of lignin staining, in contrast to the structured pattern of lignification observed in both wild-type and *eli1* tracheids. Ectopically lignified cells also stained more intensely with Toluidine Blue (Fig. 3E,G) as did the secondary wall thickenings of tracheids of *eli1* and wild-type plants (Fig. 3C).

To investigate the *eli1* phenotype in other plant organs, sections from the basal part of 6-week-old inflorescence stems were observed. The diameter of the *eli1* inflorescence stem sections (Fig. 2G) was reduced to about two-thirds of the wild-type stem diameter (Fig. 2D). Toluidine blue staining of inflorescence stem sections showed an increased number of tracheids and disruption of xylem strands in *eli1* (compare Fig. 2E, wild type, with 2H, *eli1*). In addition, the pith parenchyma cells and some cortex cells contained unusual cell structures, revealed by Toluidine Blue staining, that also stained for lignin, that were not found in wild type (Fig. 2G and 2H, *eli1*). Longitudinal sections of the *eli1* inflorescence stem revealed that lignin occurred in a mosaic surrounding small groups of cortical and pith cells (compare Fig. 2C, wild type, with Fig. 2F, *eli1*). This was also observed in the primary roots of *eli1* seedlings (Fig. 1B) and other tissues of *eli1* plants (data not shown).

Calcofluor staining of *eli1* revealed an altered distribution of cellulosic material in the cell walls of the mutant compared with wild type. Cell apices exhibited a higher intensity of

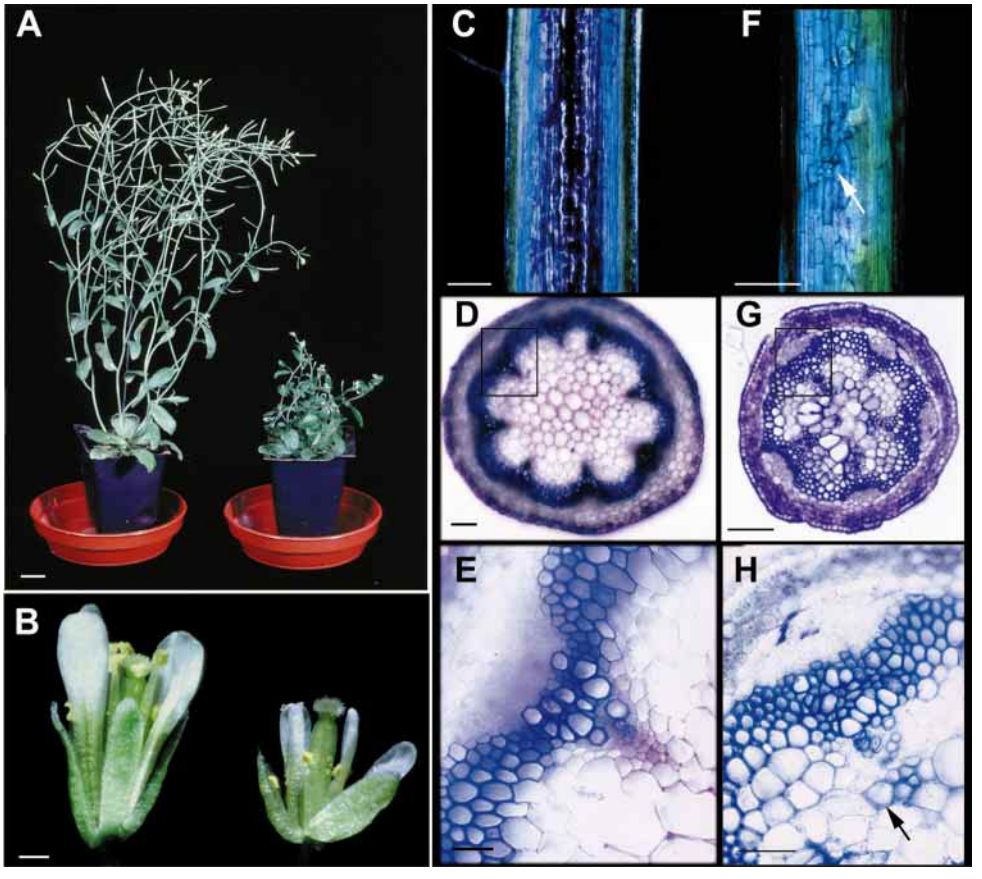

Fig. 2. Phenotypes of mature 6-week-old plants. (A) Wild-type (left) and *eli1* (right) whole plants. (B) Floral phenotype of wild-type (left) and *eli1* (right) plants. (C,D,F,G) Stem sections stained with Toluidine Blue showing xylem organization in the wild-type in longitudinal (C) and transverse (D) sections. The ectopic lignification in the pith cells in *eli1* is observed in longitudinal (F) and in transverse (G) sections. (E,H) High magnification of a vascular bundle of wild type (E) and *eli1* (H), stained with Toluidine Blue. The arrow in H indicates ectopic tracheid cells. Scale bars, 1 cm (A), 1 mm (B), 500 μm (C,F), 100 μm (D,G), 20 μm (E,H).

fluorescence (indicated by arrowheads in Fig. 8F) compared to the uniform staining observed in the wild type (Fig. 8C).

Xylem development in *eli1*

Confocal Scanning Laser Microscopy (CSLM) on the primary root of 7-day-old seedlings stained with basic fuchsin was carried out in order to determine the longitudinal organization of primary xylem in the *eli1* mutant (Fig. 4). In wild-type plants, the transition from early stages of differentiation (Fig. 4C) to later stages of differentiation (Fig. 4B) is defined by the appearance of metaxylem, shown in Fig. 4A. Projections of the CSLM optical sections of the xylem cell files revealed the alignment of xylem cells in *eli1* was severely altered (Fig. 4D,E), in that a number of individually lignified cells formed out of the xylem axis (Fig. 4E). While exhibiting the normal thickening of *Arabidopsis* metaxylem, these ectopic tracheids in *eli1* formed neither files nor perforation plates. In addition, the protoxylem cell files had irregular complex thickenings (Fig. 4E). The misshapen xylem cells in *eli1* were more isometric than their wild-type counterparts, with increased diameters and decreased length compared to the wild type (Fig. 4B,C). The Casparian strip seen in the wild type (Fig. 4B,C) was replaced in *eli1* by more strongly fluorescing amorphous deposits of lignin (Fig. 4D,E, arrowed). UV autofluorescence detection of lignin confirmed the lignification patterns observed in thin sections stained with Toluidine Blue, and in whole mounts stained with phloroglucinol.

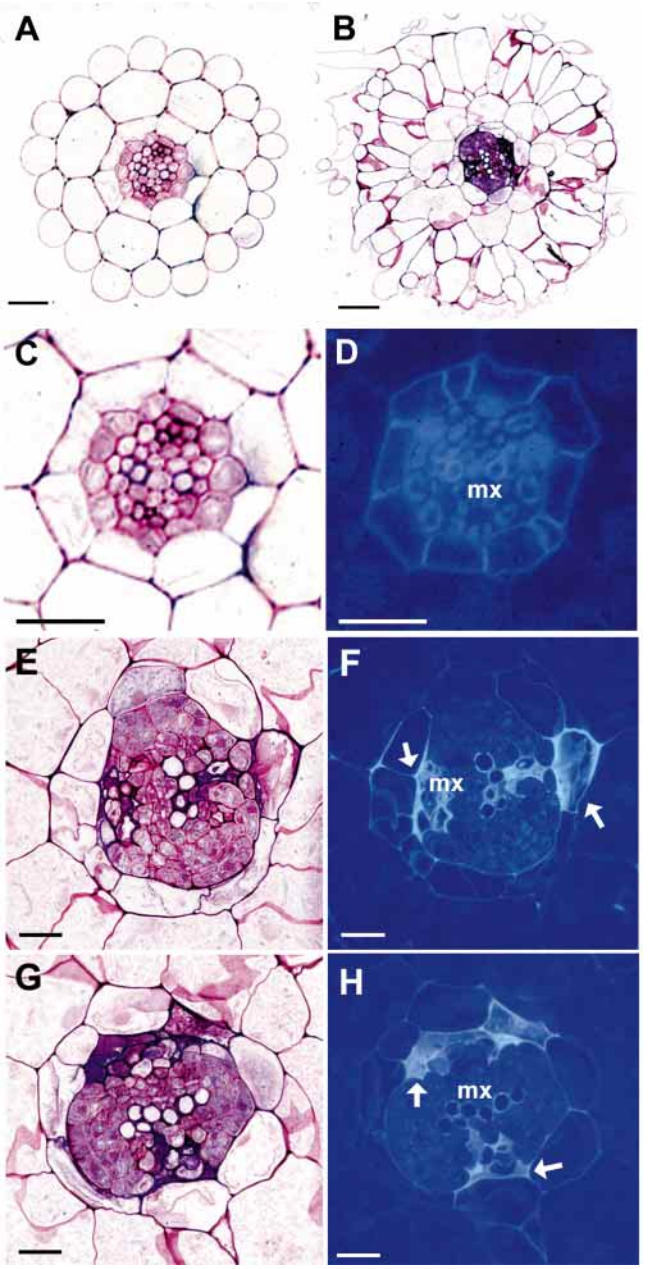

Fig. 3. Transverse sections of 7-day-old primary roots. (A,B) Whole sections of the primary root of Columbia wild type (A) and *eli1* (B) stained with Toluidine Blue. (C,E,G). 2 μm thick sections of the vascular cylinder in the differentiation zone stained with Toluidine Blue: wild type (C) and *eli1* (E,G). (D,F,H). The same sections of the vascular cylinder shown in C,E,G viewed with polarized light: wild type (D) and *eli1* (F,H). The sections shown in E and G were adjacent. Scale bars in all the images is 20 μm. mx, metaxylem. Arrowheads indicate autofluorescence.

Secondary wall formation in *eli1* seedlings

The ultrastructure of *eli1* and wild-type cell walls in transverse sections of roots of 7-day-old seedlings was investigated. Transmission electron microscopy (TEM) revealed substantial differences in the cell walls of different cell types in the *eli1* mutant (Fig. 5). In wild type, the secondary cell walls of the differentiated xylem cells were characterised by dense uranyl acetate staining (Fig. 5A). Sections of *eli1* primary roots revealed the presence of similar densely staining structures inside some non-vascular cells (Fig. 5B), but these lacked the regular striated appearance of normal secondary thickenings. To define the subcellular localisation of lignin, immunolocalization with an anti-lignin antibody, GSzt L4, which binds specifically to guaicyl and syringyl residues in maize lignin (Joseleau and Ruel, 1997), was carried out. Discrete localization of the anti-lignin antibodies to the xylem axis in wild-type roots was observed (Fig. 6B) indicating that the antibody was suitable for specifically localizing lignin in *Arabidopsis*. Preimmune sera did not show specific labelling (Fig. 6F). The pattern of antibody labelling in sections of *eli1* mutant roots revealed several non-xylem cells and other structures that contained large amounts of lignin (Fig. 6D). TEM and immunogold labelling revealed lignin was specifically localized to the secondary wall thickenings of proto- and metaxylem cells (electron-dense particles in Fig. 5C). In *eli1* roots the lignin antibody was localized to the ectopic secondary thickenings found in endodermal cells for example (Fig. 5F). In contrast, the anti-lignin antibody did not react with cell walls of an endodermal cell from wild-type roots (Fig. 5E).

Genetic interactions of *eli1* with mutants affected in xylem development and cell expansion

A number of cell expansion mutants have been described (Baskin et al., 1995; Hauser et al., 1995) which have root phenotypes related to *eli1*. Phloroglucinol staining of *lit* roots revealed an abnormal pattern of lignification similar to that seen in the primary root of *eli1*, but localised mainly to the root tip region (Fig. 8H). Genetic interactions between *eli1* and *lit* were studied to reveal relationships between these two loci. Crosses between *eli1* and *lit* mutants yielded 100% wild-type

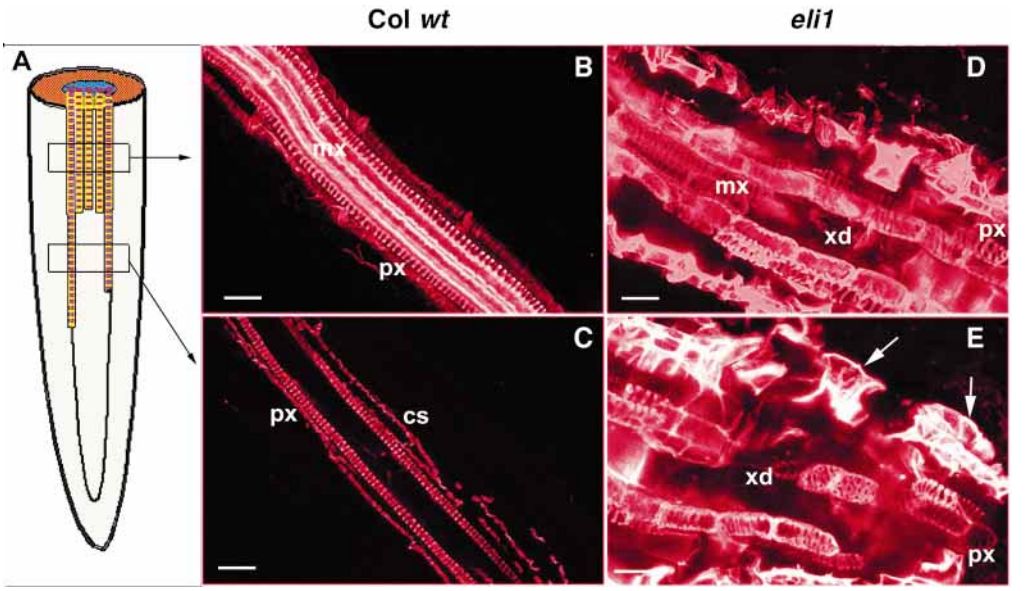

Fig. 4. Confocal microscopic visualisation of lignified tissues in 7-day-old primary root. (A) Schematic representation of xylem organization in the primary root. (B,C) Projection of Z-series images of xylem in the late differentiation zone (B) and in the early differentiation zone (C) of wild-type roots. (D,E) Projection of Z-series images of xylem in the late differentiation zone (D) and in the early differentiation zone (E) of *eli1* mutant roots. Scale bars (B,C,D,E) 10 μm. px, protoxylem; mx, metaxylem; cs, casparian strip; xd, xylem discontinuity; arrows indicates autofluorescence.

F_1 progeny and self-pollination of this F_1 progeny gave an F_2 progeny segregating in a 9:3:3:1 ratio (233 wild type: 92 *lit*:85 *eli1*: 27*eli1lit*; χ^2=2.52; P>0.05) for wt: *eli1*: *lit:* *eli1 lit* phenotypes. The F_2 segregating families of crosses between *eli1* and *lit* were grown for 7 days in media containing 30 mM sucrose, to distinguish the *lit* and *eli1* root phenotypes (Fig. 7A). The double *eli1 lit* mutant was characterized by a more extreme whole plant phenotype, with a dwarfed seedling that ultimately died at 3 weeks, and shorter fatter roots than the parental mutants. A highly compressed cell morphology was also observed in roots (Fig. 7A). Phloroglucinol staining of the *eli1 lit* double mutant (Fig. 7C) showed more extensive ectopic lignification and disruption of the vascular system than was observed in either single mutant. This was confirmed by CLSM of the primary root, which revealed severely disrupted xylem formation, with many additional single tracheids and disrupted tracheid cell files of nearly isometric cells (Fig. 7G). SEM analysis of hypocotyl epidermal cells also showed nearly isometric cells often with bulbous protrusions (arrow in Fig. 7B). These results indicate a possible additive effect of the *eli1* and *lit* mutations on cell expansion, xylem organization and ectopic lignification, and the non-viability of the double mutant revealed the importance of both genes for plant development.

The *wol* mutant is characterised by a narrower vascular cylinder composed mainly of protoxylem cell files, with no apparent metaxylem or phloem (Scheres et al., 1995). The primary defect in *wol* is thought to be the absence of a specific cell division in the stele during embryogenesis, leading to fewer vascular initials. Potential genetic interactions between *wol* and *eli1* were studied in double mutants (Fig. 7D). Analysis of roots from the F_2 segregation of the crosses showed 310 wt: 116 *wol*: 119 *eli1*: 22 *eli1wol* χ^2=4; P>0.05) corresponding to a 9:3:3:1 ratio.

Seven-day-old *eli1wol* double mutants revealed a seedling phenotype similar to the *wol* single mutant (Fig. 7E). CSLM analysis of the *eli1 wol* double mutant in 7-day-old seedlings (Fig. 7I) revealed only a few protoxylem strands in the narrow vascular cylinder, characteristic of *wol* (Fig. 7H). *eli1 wol* seedlings had reduced ectopic lignification compared to *eli1* (Fig. 7I, compare to Fig. 4D), and nearly normal cell expansion compared to the *eli1* mutant.

Cell expansion and secondary wall formation

The *lit* phenotype is conditional upon sucrose levels (Hauser et al., 1995), therefore the phenotype of *eli1* seedlings grown in media supplemented with 30 mM or 100 mM sucrose was assessed (Table 1). Growth on different sucrose concentrations had no discernable effects on either cell elongation or lignification in *eli1* seedlings. In contrast, growth of *lit* seedlings on higher sucrose levels caused reduced cell expansion and increased ectopic lignification. In addition, dark grown *lit* hypocotyls were longer than dark grown *eli1* hypocotyls and did not exhibit ectopic lignification (Table 1). This suggested a possible dependence of ectopic lignification upon cell expansion. To test this, several mutants with reduced cell expansion phenotypes were assessed for lignin content and altered cell wall composition. The *rsw1* mutant (Baskin et al., 1995; Arioli et al., 1998) is a temperature sensitive mutant of a catalytic subunit of cellulose synthase. At a restrictive temperature of 31°C *rsw1* exhibits radial swelling of the root caused by misshapen and often smaller cells, as shown in Fig. 8J,K L. Fig. 8K shows phloroglucinol-stained roots of *rsw1*, and several ectopically lignified cells are visible. The extent of ectopic lignification is not as high as that seen in *eli1* (Fig. 8E) or in *lit* (Fig. 8H). In addition to phloroglucinol staining, thin sections of roots of selected cell expansion mutants were stained with Calcofluor to reveal possible differences in cell wall composition. As shown previously in Figs 6C and 8F, *eli1* exhibited patches stained brightly by Calcofluor, and these appear to are associated with secondary-thickened walls as

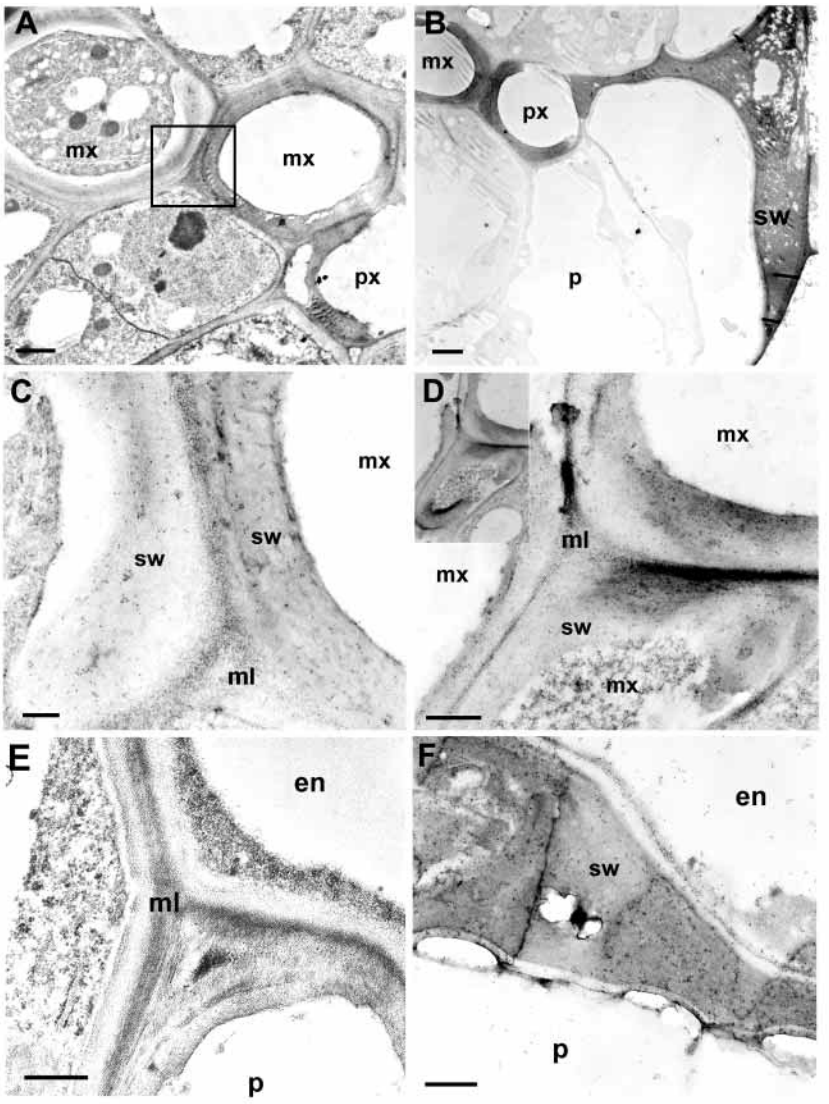

Fig. 5. Ultrastructural analysis of wild-type and *eli1* cell walls. (A,B) Transmission electron micrographs of a section from a 7-day-old root showing secondary cell wall deposition in proto- and metaxylem cells in the vascular cylinder (A). A section in the same region of the root of the *eli1* mutant shows abnormal secondary cell wall deposition (B). (C-F) Immunogold labelling with GSzt L4 antibody showing distribution of lignin. (C) Higher magnification of the boxed area in A showing specific GSzt L4 antibody labelling in the secondary walls of the xylem cell in the wild type, and in the *eli1* mutant (D); the inset in D shows an abnormal xylem cell in *eli1*; (E) micrograph showing the absence of GSzt L4 antibody labelling in non-xylem cells in the wild type and (F) GSzt L4 antibody labelling of ectopic secondary walls in endodermal cells. Px, protoxylem; mx, metaxylem; en, endodermis; p, pericycle; sw, secondary wall; ml, middle lamella. Scale bars, (A) 1 μm; (B) 2 μm; (C) 200 nm; (D,E, F) 500 nm.

shown in sections of wild-type roots (Figs 6A, 8C). Fig. 8L shows a Calcofluor-stained section of an *rsw1* root. Bright fluorescence is seen in the apices of junctions between cell walls, a pattern not seen in wild type (Fig. 8C). The *korrigan1* (*kor1*) mutation alters cell expansion in roots and hypocotyls, and is defective in an endo-1,4-β-D-glucanase (EGase) (Nicol et al., 1998). Calcofluor staining of thin sections of *kor1* roots revealed a patchy pattern similar to that observed previously (Fig. 8O; Nicol et al., 1998), and similar to that observed in *eli1* and *rsw1*. Calcofluor staining of *lit* revealed less cellulosic material in the cell walls (Fig. 8I). *kor1* also exhibited phloroglucinol staining of non-vascular cells (Fig. 8N, compared to wild type in 8B). Finally, light-grown *det3* plants exhibit reduced cell elongation and altered cell morphology due to reduced levels of a vacuolar ATPase subunit (Schumacher et al., 1999). Phloroglucinol staining of *det3* roots revealed extensive ectopic lignification (compare Fig. 8S with wild-type roots in 8B) and Toluidine Blue-stained sections of *det3* inflorescence stems revealed extensive lignification of cortical and pith cells (dark blue staining in Fig. 8R). These experiments demonstrated an association of ectopic lignification in several cell expansion mutants which are deficient in both structural components of the cell wall (cellulose synthase and an endoglucanase) and in a V-ATPase that is predicted to promote solute uptake into the vacuole and thus drive cell expansion. This suggested a linkage between cell expansion and the initiation of secondary cell wall formation and subsequent lignification.

DISCUSSION

The control of cell wall formation in higher plants plays a central role in the processes of cellular differentiation and morphogenesis. Cell walls are dynamic structures capable of expansion during cell growth, and become fixed into a final shape upon the cessation of growth (reviewed by Carpita and Gibeaut, 1993). Often the primary cell wall is further elaborated by the deposition of a secondary wall to provide additional mechanical strength and water resistance. The processes involved in determining the final shape of plant cells and subsequent secondary wall formation must be subject to multiple levels of regulation, because the processes that modify cell walls after cessation of growth are essentially irreversible. Little is known about how cell expansion is integrated with secondary wall formation.

We have identified a genetic locus, *ELI1*, that when mutated results in the production of large amounts of lignin in cells that do not normally lignify. We discuss the phenotypes associated with three independent alleles at the *eli1* locus, reveal that several other cell expansion mutants also exhibit aberrant secondary wall formation, interpret the phenotypes resulting from genetic interaction studies, and describe a possible role for *ELI1* in controlling secondary wall formation in *Arabidopsis*.

ELI1 is a novel regulator of cell expansion that promotes cell enlargement and suppresses secondary cell wall formation

Phloroglucinol staining revealed extensive lignin deposition

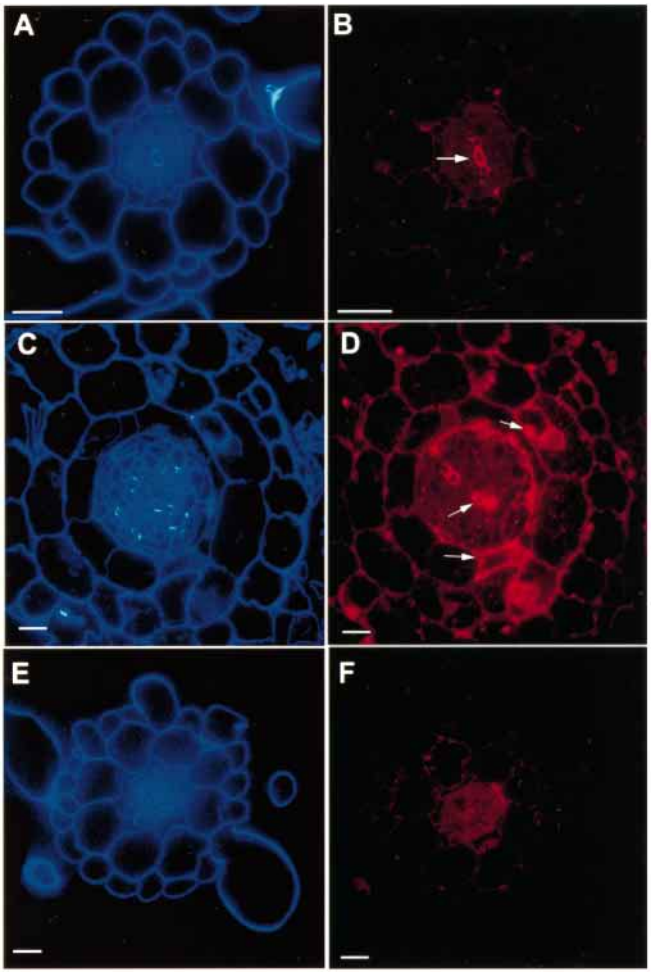

Fig. 6. Distribution of anti-lignin antibody staining in *eli1* primary root sections. Seven-day-old Col wt and *eli1* primary root sections were subjected to fluorescence immunohistochemistry with the GSzt L4 antibody to determine the distribution of lignin. (A,C,E) Calcofluor staining of wild-type (A,E) and *eli1* (C) roots to reveal cell walls. (B,D,F) Subcellular localization of the GSzt L4 antibody using cy3-labelled goat anti-rabbit antibody and immunofluorescence. (B) Wild-type lignification detected in protoxylem and metaxylem (arrow). In the *eli1* mutant (D) additional lignin is localised in endodermal and cortical cells (arrows). (F) Labelling of wild-type roots with pre-immune serum as a negative control for the specificity of the GSzt L4 antibody. Scale bar, 10 μm.

in many different cell types in the root, hypocotyl and inflorescence stem of *eli1* mutants. Unlike the sculpted patterns of lignin deposition in secondary thickenings of tracheids and fibres, the ectopic lignin characteristic of *eli1* plants occurred in amorphous patches that were not associated with specific groups of cells. Immuno-gold electron microscopy using a lignin-specific antibody identified lignin in large electron-dense bodies, typical of normal secondary thickening, in non-vascular cells of *eli1*, and in the secondary thickenings of xylem cells in both *eli1* and wild-type roots. Calcofluor staining of the cell walls of *eli1* seedlings revealed additional cellulosic deposits in non-vascular cells as well as in secondary-thickened xylem cells (compare Figs 6A with 6C, and 8C with 8F), indicating that not only additional lignin but other cell wall components are deposited aberrantly in *eli1* seedlings. Electron microscopy revealed that these deposits are remarkably similar in structure (although distributed differently in cells as described above) to normal secondary thickening in xylem cells, supporting the interpretation that secondary wall

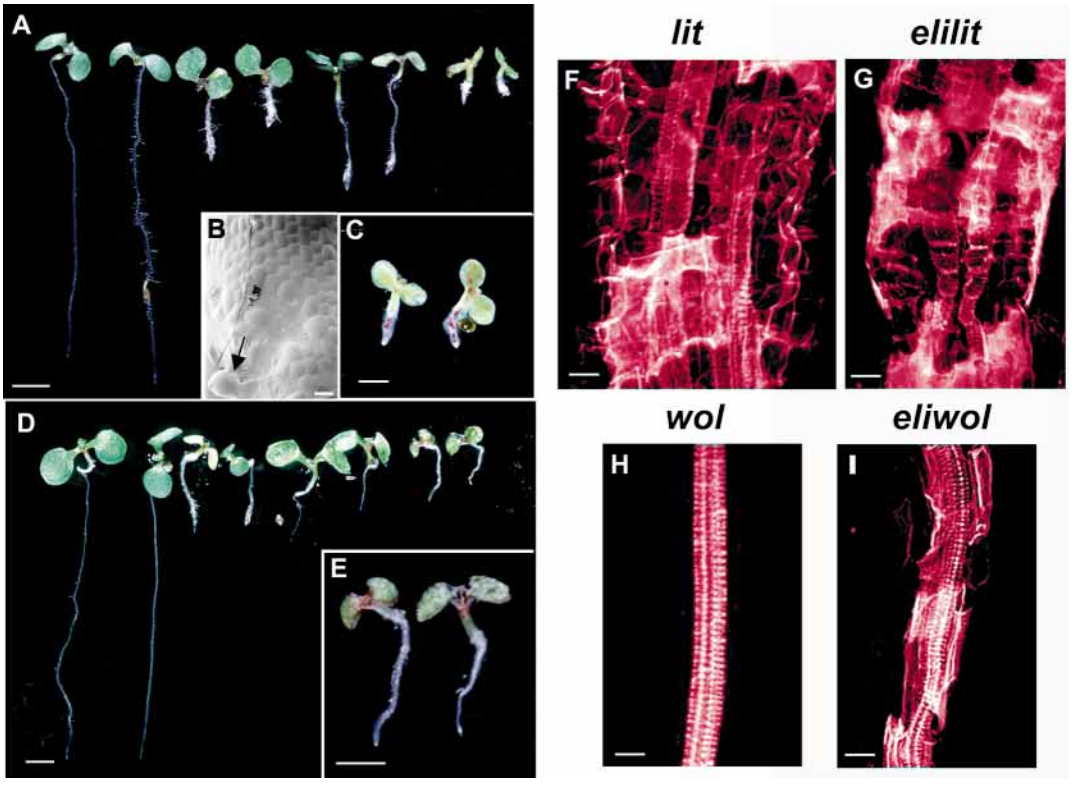

Fig. 7. Double mutant phenotypes. (A) Seven-day-old seedlings of (from left to right in pairs) wild type, *eli1*, *lit*, and *eli1 lit* double mutant. (B) Scanning electron micrograph of 7-day-old dark germinated hypocotyl cells of the *eli1lit* double mutant. (C) Phloroglucinol staining of *eli1 lit* double mutant seedlings. (D) Seedling phenotypes of (from left to right) wt, *eli1*, *wol*, and *eli1 wol* double mutant. (E) Higher magnification of *eli1 wol* double mutant phenotype. (F,G,H,I) Confocal images of lignified tissues in the primary root in *lit* (F); *eli1 lit* double mutant (G), *wol* (H) and *eli1 wol* double mutant (I). Scale bars, (A,D,E) 10 mm; (B) 50 μm; (C) 5 mm; (F,G,H,I) 10 μm.

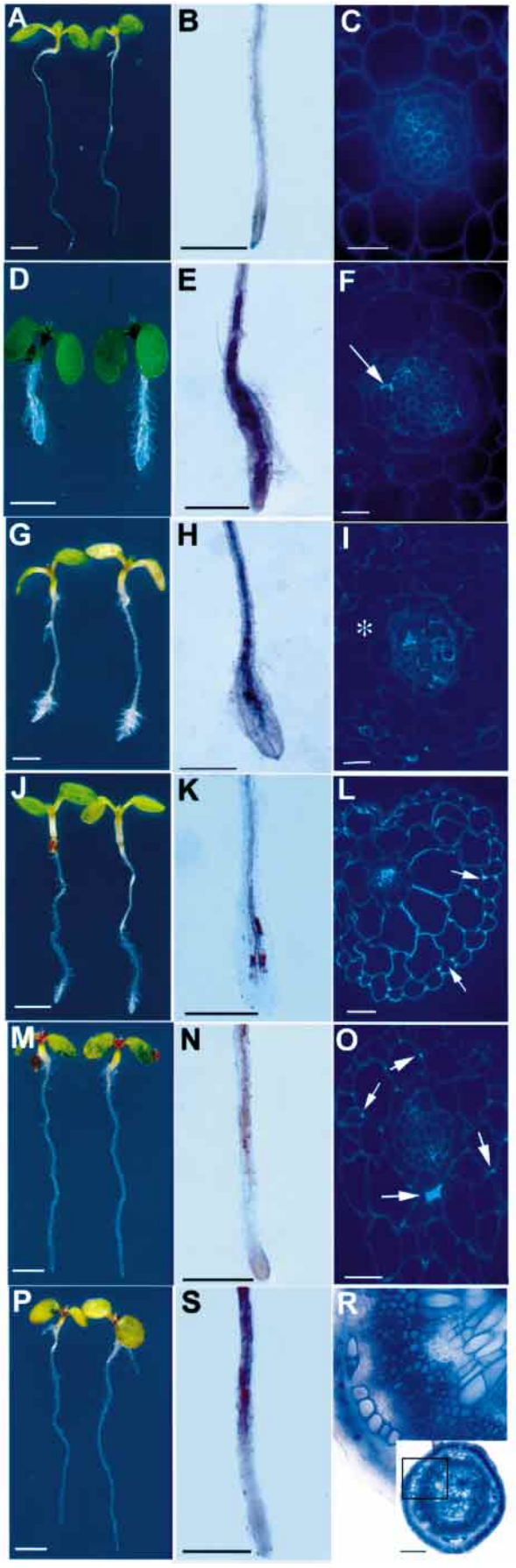

Fig. 8. Patterns of lignification and cellulose deposition in cell expansion mutants. (A,D,G,J,M,P) Seven-day-old seedlings of Col wild type (A), *eli1* (D), *lit* (G), *rsw1* (J), *kor1* (M), *det3* (P) germinated on 30 mM sucrose. Seedlings were germinated and grown for 7 days at 21°C, except *rsw1*, which was grown for 5 days at 21°C and then transferred to 31°C for 2 further days. (B,E,H,K,N,S) Phloroglucinol staining of the root of wild type (B), *eli1* (E), *lit* (H), *rsw1* (K), *kor1* (N), *det3* (S) showing different patterns of lignification. (C,F,I,L,O) Calcofluor staining of cell walls in wild type (C), *eli1* (F), *lit* (I), *rsw1* (L), and *kor1* (O) primary roots. The asterisk in I indicates reduced Calcofluor staining. The arrows indicate areas of increased Calcofluor staining. (R) Stem transverse section stained with Toluidine Blue showing xylem organization in the *det3* mutant similar to the one observed in *eli1*. The higher magnification of a vascular bundle shows the ectopic lignification of the pith cells in *det3*. Scale bars, (A-Q) 10 mm, (R) 20 μm.

formation, and not specifically lignin synthesis and deposition, is de-regulated in *eli1* plants.

The role of *ELI1* in xylem development

In cells destined to form xylem, the same cell expansion defect is manifest in *eli1* and *lit* plants, and in addition tracheids are more heavily lignified, cell files are disrupted and there are more tracheid cells. These effects appear additive in the *eli1 lit* double mutant, with severely disrupted xylem and many near-isodiametric tracheids, leading to death several weeks after germination. These results suggested that the *ELI1* gene product may also be involved in specifying xylem vessel development.

To test this hypothesis, interactions between *eli1* and *wol*, a mutation that alters xylem specification, were studied. The primary defect in wol plants is thought to be the absence of specific cell divisions during axis formation (Scheres et al., 1995) resulting in the loss of metaxylem and phloem cells in the primary root. The *eli1 wol* double mutant phenotype is of near-normal cell expansion, continuous xylem files, absence of metaxylem and reduced ectopic lignification. This suggests that *ELI1* and *WOL* gene products may interact additively with respect to cell elongation and ectopic lignification, because of near-normal cell elongation and reduced ectopic lignification. This supports the interpretation derived from *eli1 lit* double mutants, that a primary defect in *eli1* is in cell expansion, as the near-wild-type cell expansion seen in the *eli1 wol* double mutant leads to reduced ectopic lignification of non-xylem cells. The continuous xylem strands typical of *wol* in the double mutant indicates that *wol* is epistatic to *eli1* with respect to this phenotype. This may indicate a separate role for *ELI1* in promoting formation of continuous xylem strands during tracheid formation. An alternative explanation of this epistasis is that the defect in *wol* plants, the absence of progenitor metaxylem cells, occurs earlier in development than the defect in *eli1* plants.

Aberrant secondary cell formation is exhibited by other cell expansion mutants

Another cell expansion mutant, *lit*, also displays ectopic lignification. This phenotype is associated with the extent of cell expansion in *lit*, shown by the dependent of cell expansion and lignification on external sucrose levels. Analysis of double *eli1 lit* mutants revealed an additive phenotype of significantly

shorter, almost isodiametric cells with increased ectopic lignification, indicating that *ELI1* and *LIT* may act in parallel in at least two independent mechanisms governing normal cell expansion. These observations strongly suggest that reduced cell expansion in *eli1* leads to ectopic secondary thickening and lignification. In this model the *ELI1* gene product acts to promote cell size increase and inhibit secondary thickening and subsequent lignification in non-xylem cells. The observation that *ELI1* acts during later stages of development, such as in the elongation zone of the primary root, is consistent with this proposed role of the *ELI1* gene product in normal cell expansion.

Ectopic lignification was also observed in *rsw1*, defective in a catalytic subunit of cellulase synthase (Arioli *et al*, 1998), in *korrigan*, defective in a plasma membrane associated β-1,4 endoglucanase (Nicol et al., 1998), and in *det3* (Schumacher et al., 1999), with reduced vacuolar ATPase levels. The varying degree of ectopic lignification observed in these mutants was correlated with the degree of altered cell expansion, suggesting a meaningful link between these processes. This linkage was clearly demonstrated by the temperature dependence of both cell expansion and ectopic lignification in the *rsw1* allele.

However, ectopic lignification is not an inevitable consequence of reduced cell expansion, because several cell expansion mutants such as *pom-pom* and *cobra* (Hauser et al., 1995) do not exhibit ectopic lignification (unpublished data). Therefore specific features of mutants such as *eli1*, *lit*, *rsw1* and *korrigan* lead to the induction of inappropriate secondary wall formation and lignification.

Mutations in the cellulose synthase gene *RSW1* (Arioli et al., 1998) cause severe alterations in cell shape due to disassembly of cellulose synthase complexes and consequent accumulation of non-crystalline cellulose in the primary cell wall. The β-1,4 endoglucanase encoded by *korrigan* is required for the correct assembly of the cellulose-hemicellulose network in expanding primary walls. The V-ATPase encoded by *DET3* may regulate cell expansion by controlling solute uptake into the vacuole that drives osmosis, the motive force for cell expansion. The additive effect of *lit* and *eli1* indicate there are at least two independent mechanisms modulating the attainment of normal cell volume, consistent with the need for multiple components for normal cell expansion described above. These postulated regulatory mechanisms require the components and forces driving expansion of the cell wall to be monitored and integrated to maintain the correct geometry of the primary wall. This study demonstrates that this postulated mechanism(s) may also signal differentiation pathways such as lignification, which is normally only initiated in specific cells that have reached a defined shape and size, such as tracheids. Brassinosteroids regulate *korrigan* transcription (Nicol et al., 1998) and have been postulated to affect V-ATPase function (Schumacher et al., 1999), and also promote secondary wall formation in differentiating tracheids (Yamamoto et al., 1997). They are therefore candidates for integrating cell size and differentiation. However, initial experiments have not yet demonstrated a dependence of cell size and ectopic lignin formation on exogenous brassinosteroids or other growth regulators such as auxin, gibberellins, ethylene or cytokinins in *eli1* and other expansion mutants (data not shown). Consequently, the identification of the *ELI1* gene and determination of its function will provide important new insights into the mechanisms integrating morphogenesis and differentiation.

We are grateful to Marie-Theres Hauser, Philip Benfey, Herman Höfte and Joanne Chory for providing mutant lines, Katia Ruel and Jean-Paul Joseleau for providing anti-lignin antibodies, and Brian Wells, Pablo González-Melendi and Kim Findlay for their valuable help with microscopy. We thank Liam Dolan for comments on the manuscript, advice and encouragement. A. I. C.-D. was supported by a PhD Studentship from the John Innes Foundation.

REFERENCES

Arioli, T., Peng, L., Betzner, A. S., Burn, J., Wittke, W., Herth, W., Camilleri, C., Höfte, H., Plazinski, J., Birch, R., Cork, A., Glover, J., Redmond, J. and Williamson, R. (1998). Molecular analysis of cellulose biosynthesis in Arabidopsis. *Science* **279**, 717-20.

Baskin, T., Herth, W., Cork, A., Birch, R., Rolfe, J., Redmond, J. and Williamson, R. (1995). Root morphology mutants in Arabidopsis thaliana. *Austr. J. Plant Physiol.* **19**, 427-437.

Bell, C. J. and Ecker, J. R. (1994). Assignment of 30 microsatellite loci to the linkage map of Arabidopsis. *Genomics* **19**, 137-144.

Berleth, T. and Jürgens, G. (1993). The role of the *monopteros* gene in organizing the basal body region of the *Arabidopsis* embryo. *Development* **118,** 575-587.

Bonin, C. P., Potter, I., Vanzin, G. F. and Reiter, W. D. (1997). The MUR1 gene of Arabidopsis thaliana encodes an isoform of GDP-D- mannose-4,6-dehydratase, catalyzing the first step in the de novo synthesis of GDP-L-fucose. *Proc. Natl. Acad. Sci. USA* **94,** 2085-2090.

Cabrera y Poch, H.L., Peto, C. A. and Chory J. (1993). A mutation in the Arabidopsis *DET3* gene uncouples photoregulated leaf development from gene expression and chloroplast biogenesis. *Plant J.* **4**, 671-682.

Carpita, N. C. and Gibeaut, D. M. (1993). Structural models of primary cell walls in flowering plants: consistency of molecular structure with the physical properties of the walls during growth. *Plant J.* **3,** 1-30.

Cosgrove, D. (1993). How do plant cell walls extend? *Plant Physiol.* **102,** 1-6.

Cosgrove, D. (1999). Enzymes and other agents that enhance cell wall extensibility. *Annu. Rev. Plant Physiol. Plant Mol. Biol.* **50,** 391-415.

Dharmawardhana, D. P., Ellis, B. E. and Carlson, J. E. (1995). Characterization of vascular lignification in *Arabidopsis thaliana*. *Can. J. Bot.* **70,** 2238-2244.

Fukuda, H., Ito, M., Sugiyama, M. and Komamine, A. (1994). Mechanisms of the proliferation and differentiation of plant cells in cell culture systems. *Int. J. Dev. Biol.* **38,** 287-299.

Hauser, M.-T., Morikami, A. and Benfey, P. N. (1995). Conditional root expansion mutants of *Arabidopsis*. *Development* **121,** 1237-1252.

Joseleau, J. P. and Ruel, K. (1997). Study of lignification by non-invasive techniques in growing maize internodes. An investigation by Fourier transform infrared cross-polarization-magic angle spinning ^{13}C-nuclear magnetic resonance spectroscopy and immunocytochemical transmission electron microscopy. *Plant Physiol.* **114,** 1123-1133.

McCann, M. and Roberts, K. (1994). Changes in cell wall architecture during cell elongation. *J. Exp. Bot.* **45,** 1683-1691.

Nicol, F., His, I., Jauneau, A., Vernhettes, S., Canut, H. and Höfte, H. (1998). A plasma membrane-bound putative endo-1,4-β-D-glucanase is required for normal wall assembly and cell elongation in *Arabidopsis*. *EMBO J.* **17,** 5563-5576.

O'Brien, T. P. (1981). The primary xylem. In *Xylem Cell Development* (ed. J. Barnett), pp. 14-46. Turnbridge Wells: Castle House Pub.

Pear, J. P., Kawagoe, Y., Schreckengost, W. E., Delmer, D. and Stalker, D. M. (1996). Higher plants contain homologs of the bacterial *celA* genes encoding the catalytic subunit of cellulose synthase. *Proc. Nat. Acad. Sci. USA* **93,** 12637-12642.

Roberts, K. (1989). The plant extracellular matrix. *Curr. Opin. Cell Biol.*, 1020-1027.

Scheres, B., Di Laurenzio, L., Willemsen, V., Hauser, M.-T., Janmaat, K., Weisbeek, P. and Benfey, P. N. (1995). Mutations affecting the radial organisation of the *Arabidopsis* root display specific defects throughout the embryonic axis. *Development* **121,** 53-62.

Schneider, K., Wells, B., Dolan, L. and Roberts, K. (1997). Structural and

genetic analysis of epidermal cell differentiation in *Arabidopsis* primary roots. *Development* **124,** 1789-1798.

Schumacher, K., Vafeados, D., McCarthy, M., Sze, H, Wilkins, T. and Chory, J. (1999). The Arabidopsis *det3* mutant reveals a central role for the vacuolar H-ATPase in plant growth and development. *Genes Dev.* **13**, 3259-3270.

Taylor, N. G., Scheible, W. R., Cutler, S., Somerville, C. R. and Turner, S. R. (1999). The irregular xylem3 locus of Arabidopsis encodes a cellulose synthase required for secondary cell wall synthesis. *Plant Cell* **11,** 769-780.

Turner, S. R. and Somerville, C. R. (1997). Collapsed xylem phenotype of Arabidopsis identifies mutants deficient in cellulose deposition in the secondary cell wall. *Plant Cell* **9,** 689-701.

Wardrop, A. B. (1981). Lignification and xylogenenis. In *Xylem Cell Development* (ed. J. Barnett). Tunbridge Wells: Castle House Publishing.

Wells, B. (1985). Low temperature box and tissue handling device for embedding biological tissue for immunostaining in electron microscopy. *Micron and Microscopica Acta* **16,** 49-53.

Wisman, E., Cardon, G. H., Franz, P. and Saedler, H. (1998). The behaviour of the autonomous maize transposable element En/Spm in *Arabidopsis thaliana* allows efficient mutagenesis. *Plant Mol. Biol.* **37,** 989-999.

Yamamoto, R. Demura, T and Fukuda, H. (1997). Brassinosteroids induce entry into final stage of tracheary element differentiation in cultured *Zinnia* cells. *Plant Cell Physiol.* **38,** 980-983.

Zhong, R., Taylor, J. and Ye, Z.-H. (1997). Disruption of interfascicular fiber differentiation in an Arabidopsis mutant. *Plant Cell* **9,** 2159-2170.

Zhong, R. and Ye, Z. H. (1999). *IFL1*, a gene regulating interfascicular fiber differentiation in Arabidopsis, encodes a homeodomain-leucine zipper protein. *Plant Cell* **11,** 2139-2152.